VOL. 14, NO. 2, JANUARY 2019 ISSN 1819-6608
ARPN Journal of Engineering and Applied Sciences

www.arpnjournals.com

RMS CURRENT BASED PASSIVE ISLANDING DETECTION OF DG USING ADAPTIVE LINEAR NEURAL NETWORK

Anu Radha and Shimi S. L
Electrical Engineering Department, National Institute of Technical Teachers Training and Research, Chandigarh, India
E-Mail: anuradha.elect@nitttrchd.ac.in

ABSTRACT

Distributed generators (DG) are gaining more attention in present century due to reliability and better power quality. With the increase in the use of DG, the nature of distribution is changing which causes technical issues. One of these issues is related to islanding detection. A real-time islanding detection based on ADALINE and d-q Theory is proposed in this paper. Five ADALINE neural networks are used to evaluate RMS current in d-q frame and one of these ADALINE is used to evaluate the phase angle in d-q frame using phased-locked loop (PLL). Change in RMS value of current is compared with threshold limit to detect islanding. Islanding detection unit is used to send a trip signal to DG side circuit breaker to disconnect the DG from load in case of islanding. Simulation results are validated using the real-time HIL OP4510 at different load conditions.

Keywords: ADALINE, artificial neural network, PCC, passive islanding detection technique, PLL, RMS current.

1. INTRODUCTION

NOWDAYS environment and energy- related problems are of more concern in society. Use of clean or renewable source of energy to replace fossil form of energy or traditional form of non-renewable energy is an inescapable pattern of social improvement (Qahouq 2014; Park 2013). Renewable energy in form of wind and solar energy have more potential in terms of space and development. It is well known that there is a natural complementary characteristic of wind energy and solar energy in time and space. By effectively combining solar energy and wind energy not only enhance reliability of power supply, yet additionally make full utilization of a variety of clean energy augmenting hybrid wind and solar system for power generation (Akyuz 2012; Hakimi 2009; Rehman 2012). DG has negative impact on main grid when connected directly because most DG sources are intermittent. DG contained in microgrid supports each other i.e. work as complementary. By using integration of various distributed resources, loads and controllable load, dependency on main grid can be reduced. i.e. for sustainable energy development, microgrid is a critical part.

Different strategies are used when DG operates off-grid or on-grid and grid-connected mode or islanding mode. Later on, numerous little limit DG control frameworks have been fused into the utility power grid. The small units of DG control frameworks are straightforwardly joined into the main grid for providing electric energy to loads. Traditionally, there are some insurance strategies for the DG control frameworks, including the recognition of grid power quality and are landing mode. An operation supposed "islanding mode" is the place when DG control framework still supplies electric power to the load while the main grid is switch off because of fault or maintenance of main grid (Chowdhury 2011; Balaguer 2011). In like manner, this may cause the DG control framework providing electric power independently. Numerous issues caused by the islanding mode are:

a) Islanding mode may imperil open security or endanger maintenance laborers;
b) Islanding mode may result, unregulated voltage and frequency of electric energy of the DG control framework so the electrical hardware might be harmed;

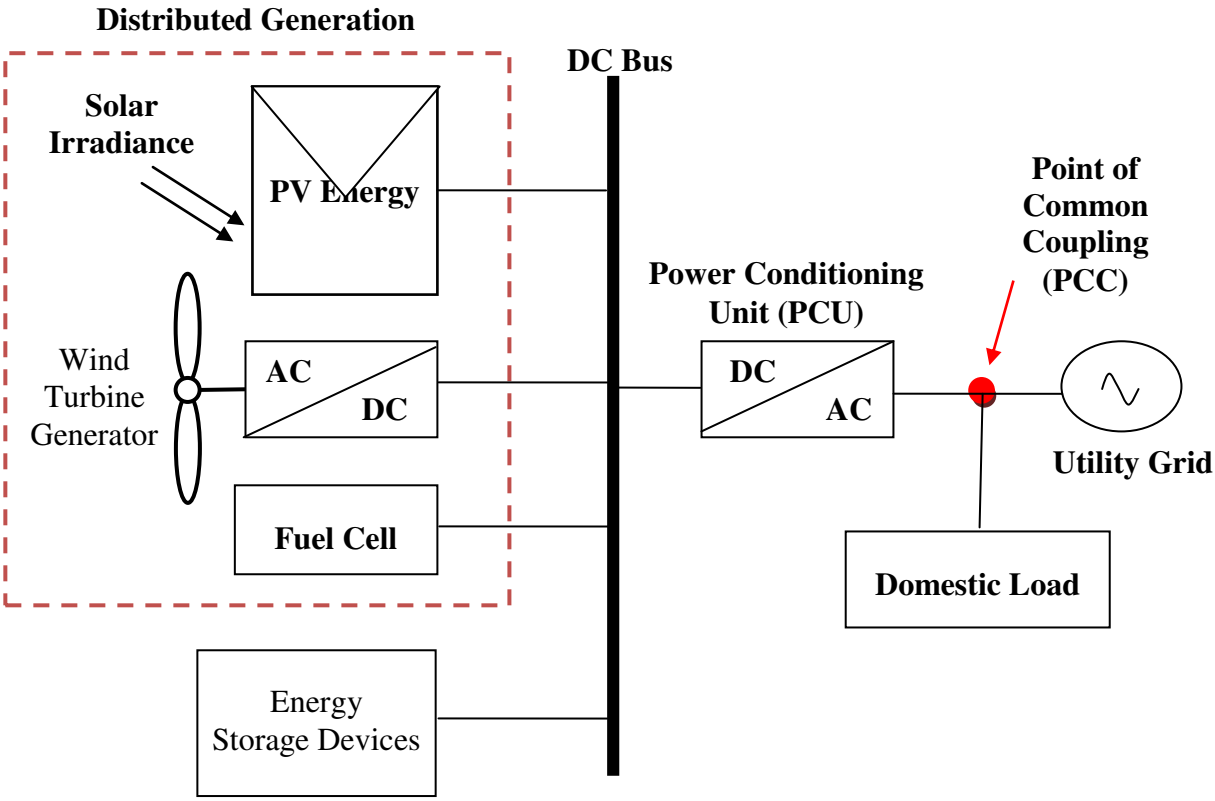

Figure-1. Block diagram of micro-grids connected to main grid.

c) Islanding mode may result, glitch of protective relay;
d) When the main grid is reconnected, islanding mode may cause non-concurrent issues for the DG control frameworks and the utility.

Henceforth, numerous islanding control measures, for example, UL1741-2000 [8], IEEE1547.1-2005 [9] and IEEE929-2000 [10] have been built up in Europe, United States of America, Japan and different nations.

Unintentional and intentional islanding are types of islanding. Where intentional islanding detection technique (IDT) can be further divided into passive islanding detection technique (PIDT), active islanding detection technique (AIDT) and communication islanding detection technique (CIDT). The PIDT are utilized to identify the difference in parameters in DG control framework for deciding if the islanding operation happens. For instance, the latent strategies incorporate a system frequency based ID, a voltage amplitude based ID (Mango 2006), and a harmonic detection based ID (Mozina 2001). If the power provided from the DG control framework is the same as the power requested by the load, both amplitude and frequency won't change. In this condition, these PIDT can't identify the islanding mode, and this non-detection of islanding is known as the "non-detection zone (NDZ)". As needs be, these latent PIDT can't meet the prerequisites of the ID control models.

With regards to the AIDT, it is utilized as a part of inverter interfaced DG control framework, named as inverter based DG control framework, and a little disturbance is fused with the yield current to infuse into the utility (Affonso 2005; Geng 2011; Mango 2006; Hung 2003; Huang 2001; Ropp 2000; Kobayashi 1994; Bahrani 2011). At the point when the utility is ostensible, the little disturbance brings about a dismissed difference in load voltage in light of the fact that the utility is exceptionally solid. On the other hand, when the utility is interfered with, the little modification can cause an awesome change in PCC frequency or PCC voltage amplitude. Along these, an assurance transfer can instantly identify a change and termed it as an islanding operation. In a split second, the inverter-based DG control framework must be disengaged from the utility in order to abstain from islanding operation. By these PIDT must agree to all global islanding control principles, with the end goal to aggregate harmonic distortion of a yield current provided from the inverter based DG control framework must be under 5% (Bahrani 2011). Thus, the change coming about because of these AIDT must be limited by the ID models with the goal that the location time of islanding identification is expanded. Be that as it may, there is a NDZ as yet existing in some AIDT. Moreover, a control technique utilized in the inverter-based DG control framework with these AIDT might be complex.

The CIDT for distinguishing the islanding operation are chiefly in light of observing the condition of circuit breakers and switches and trip the utility associated inverter when the utility is detached (Ropp 2000; Ropp 2006). In any case, these techniques are more costly and intricacy than other islanding location strategies because the extra equipment for CIDT is required.

A new enhanced ADALINE method for online ID is proposed in this paper. A new PIDT is developed based on ADALINE algorithms for estimation of symmetrical RMS current and phase angle using IPT (instantaneous power theory) (Akagi 2007; Nguyen 2009). IPT also known as p-q theory uses clarke transformation, which transforms voltage and current signals of 3-phase into the stationary reference frame or αβ.

This paper consists of 5 sections. Section II shows state of art of ANN in which different ANN types are discussed for islanding detection. Section III discusses ADALINE algorithm for estimation of symmetrical current component and phase-angle by using IPT. Section IV shows simulation result and discussion based on 5 different load cases. Final conclusion of paper includes in section V.

2. STATE OF ART OF ANN

ANNs have been effectively utilized as a part of a few building applications. Lately, this computerized reasoning method has been progressively utilized as a part of the electrical supply field (Bose 2007).

An ANN is a network of neurons or nodes comparable to the neural connection in biological system. Generally for issues related to power system, Multi-layer feed forward networks are embraced. For IDT application, ANN and its different types are applied by various research scholars in few past years. ANN based IDT has been proposed for DG with multiple inverter (Fayyad 2010) and DG with hybrid inverter (ElNozahy 2011). For IDT parameters utilized are transients in PCC voltage (Fayyad 2010) and transients in PCC current (ElNozahy 2011). Both proposed IDT are PIDT as power signals are not distorted in these techniques. For ID (islanding detection) information is extracted by using discrete wavelet transform and this information is further used to train ANN to separate islanding and non-islanding event (Fayyad 2010; ElNozahy 2011).

Another PIDT based on ANN for DFIG is proposed in (Abd-Elkader 2014). Proposed PIDT is based on measurement of symmetrical components of harmonics. By using Fourier Transform these 2nd order harmonics of current and voltage are processed and send to ANN for training. Harmonic parameter estimation debased by stochastic noise is difficult for delivered power screening. To evaluate the harmonic segments in a distorted form of power, Fast Fourier Transform (FFT) is regularly utilized (Girgis 1991). FFT based method endures from leakage effect. Also endures from determining inter harmonics, sub-harmonics and frequency deviations, its execution profoundly decreases.

To conquer the above disadvantages, LS (Least Square) and RLS (Recursive Least Square) algorithms have been used (Bettayed 1998; Pradhan 2005). These algorithms are useful for estimation of frequency but not useful for estimation of phase and amplitude. For harmonic component extraction in distorted power signal, KF (Kalman Filter) (Dash 1996) is robust technique. KF is unable to detect sudden or instantaneous changes in signals like phase, amplitude or frequency. For detection of sudden changes in signals GA (Genetic Algorithm) is used. For harmonic component extraction in distorted power signal GA is applied (Bettayed 2003). But convergence time is larger for estimation of harmonic components using GA. For estimation of harmonics, above techniques faces issues related to slow convergence, not able to detect sudden changes are overcome by using ADALINE (Adaptive Linear Neural Network) in (Dash 1996; Joorabian 2008; Sarkar 2011; Marie 2004).

ADALINE is preferred these days due to its ability to detect any dynamic changes in the system like changes in phase or amplitude or harmonics of changing amplitude or phase. Therefore ADALINE is useful for on-line adaptation. In [simulation of islanding] a new PIDT based on ADALINE algorithm is proposed (Al-Wadie 2013). In this method ADALINE is used for fast estimation of voltage angle and proposed method is independent of load power factor. In EHV transmission line for online fault detection, ADALINE is proposed (Yousfi 2010). The ADALINE is used for fundamental and dc component detection in current signal during faults. In (Yousfi 2012) proposed a new approach for an adaptive fault classifier using ADALINE. Proposed module is used to extract phase angles and symmetrical components of current in EHV lines. These estimated phase angles are used for fault classification. Proposed ADALINE based method is able for online parameter varying adaptation.

This state of art shows application of ANN for islanding detection. ANN methods used are FFT, GA, Kalman filter which having drawbacks of slow convergence speed, high computational cost and FFT failed in case of dynamic signals. While ADALINE has low computational cost, fast convergence speed and has ability of quick detection of changes in signal in dynamic environment as it has single neuron structure.

Following these advantages of ADALINE, it is used for proposed PIDT. Five different ADALINES are developed in which 4 are used for estimation of symmetrical current component of direct axis and 1 is used for phase angle estimation. Estimation of phase angle is followed by use of PLL (phase-locked loop).

3. ADALINES FOR ISLANDING DETECTION

A. d-q Current computation

Instead of positive, negative and zero terms, direct, quadrature and homopolar terms are used respectively. IPT is used to extract the d-q components of current. p-q powers are calculated according to IPT theory, and these powers are further separated in average power and oscillating power (Yousfi 2012). To compute direct and quadrature components of three phase current, direct and quadrature terms of average power are used respectively i.e. $\bar{p}_d$, $\bar{q}_d$ and $\bar{p}_q$, $\bar{q}_q$. Direct and quadrature current component extraction is shown in Figure-2.

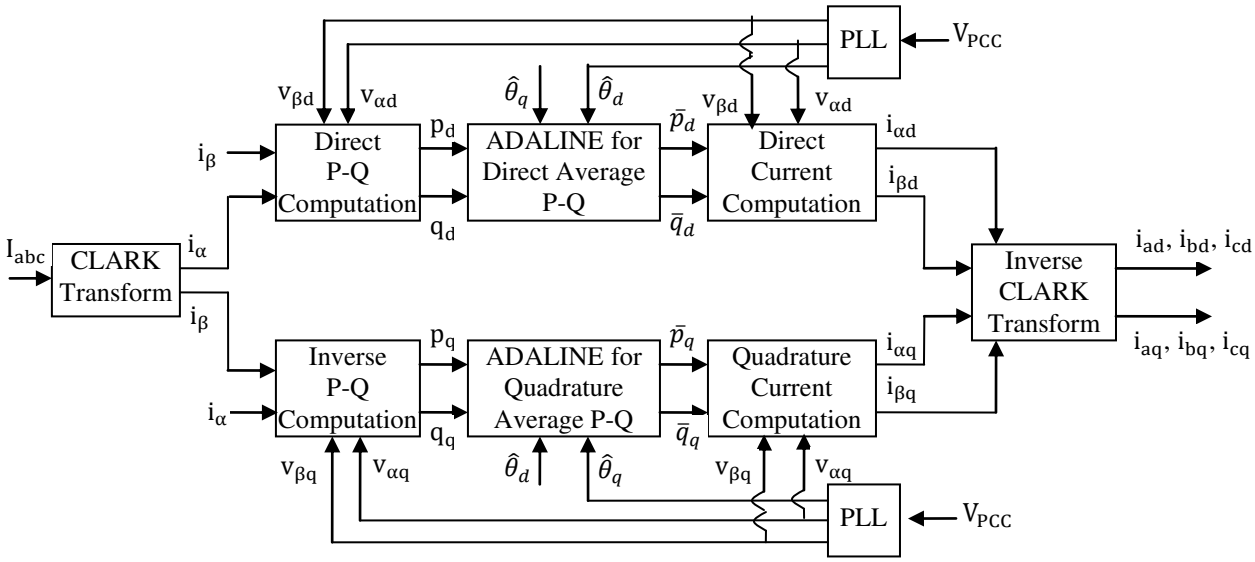

Figure-2. Block diagram of the direct and quadrature component extraction using ADALINES for the system under study.

We consider following 3-phase current, i

$$i = \sum_{k=1}^{K} \begin{pmatrix} \sqrt{2} I_{dk} C_{32} P(k\theta_d)[1\ 0]^T + \\ \sqrt{2} I_{qk} C_{32} P(-k\theta_q)[1\ 0]^T \\ +\sqrt{2} I_{hk} C_{31} cos(k\theta_h) \end{pmatrix} \quad (1)$$

Where the index d, q, h means direct, quadrature, and homopolar sequences. $P(k\theta_i)$ is the Park Matrix, C_{32} and $C_{31}$are the Clarke Matrix, k is the harmonic range, $\theta_i = \omega_i t + \delta_i$ is the current instantaneous phase with i=d, q, h, $\omega_i = 2\pi f$ is the frequency, and δ_i is the initial phase. I_{dn}, I_{qn} and $I_{hn}$are the direct, quadrature, and homopolar current amplitudes.

Similarly 3-phase voltage can be defined by replacing θ_i with phase shift between voltage and current.

Instantaneous power in IPT are calculated in the αβ frame as,

$$\begin{bmatrix} p \\ q \end{bmatrix} = \begin{bmatrix} v_\alpha & v_\beta \\ v_\beta & -v_\alpha \end{bmatrix} \begin{bmatrix} i_\alpha \\ i_\beta \end{bmatrix} \quad (2)$$

With ,

$$\begin{bmatrix} i_\alpha \\ i_\beta \end{bmatrix} = \sqrt{\frac{2}{3}} C_{32}^{T} . i$$

$$= \sum_{k=1}^{K} \begin{pmatrix} \sqrt{3} I_{dk} P(k\theta_d)[1\ 0]^T \\ +\sqrt{3} I_{qk} P(-k\theta_q)[1\ 0]^T \end{pmatrix} \quad (3)$$

Active power p is given by,

$$p = \bar{p}_d + \bar{p}_q + \tilde{p}_d + \tilde{p}_q + \tilde{p}_{dq} + \tilde{p}_{qd} \quad (4)$$

Where $\bar{p}_d$ is the direct average active power, $\bar{p}_q$ is the quadrature average active power, $\tilde{p}_d$ is the direct oscillating active power. $\tilde{p}_q$ is the quadrature oscillating active power, $\tilde{p}_{dq}$ and $\tilde{p}_{qd}$ are the direct and quadrature oscillating active power respectively.$\bar{p}_d$ and $\tilde{p}_d$ have been resulted from the direct component of currents and voltages. $\bar{p}_q$ and $\tilde{p}_q$ have been resulted from the inverse components of currents and voltages. Similarly, reactive power q is calculated by direct and quadrature components of voltage and current.

The fundamental direct currents in the αβ frames are deduced from (2) as,

$$\begin{bmatrix} i_{\alpha d} \\ i_{\beta d} \end{bmatrix} = \frac{1}{v_{\alpha d}^2 + v_{\beta d}^2} \begin{bmatrix} v_{\alpha d} & v_{\beta d} \\ v_{\beta d} & -v_{\alpha d} \end{bmatrix} \begin{bmatrix} \bar{p}_d \\ \bar{q}_d \end{bmatrix} \quad (5)$$

For direct current extraction, the amplitude of direct voltages $v_{\alpha d}$ and $v_{\beta d}$ can be arbitrarily chosen. By the phase-locked loop (PLL) circuit, instantaneous phase $\hat{\theta}_d$ is estimated to derive direct voltages. These direct voltage are given by,

$$\begin{bmatrix} v_{\alpha d} \\ v_{\beta d} \end{bmatrix} = \begin{bmatrix} \cos(\hat{\theta}_d) \\ sin(\hat{\theta}_d) \end{bmatrix} \quad (6)$$

The direct and quadrature powers are estimated by ADALINE in next section. Thus, by converting the powers in the αβ current space, the i_{ad}, i_{bd}, i_{cd}direct current components are recovered as,

$$[i_{ad} \quad i_{bd} \quad i_{cd}]^T = \sqrt{\frac{2}{3}} C_{32} [i_{\alpha d} \quad i_{\beta d}]^T \quad (7)$$

B. ADALINE neural network for d-q power calculation

To compute the auxiliary powers p_d and q_d:

$$\begin{bmatrix} p_d \\ q_d \end{bmatrix} = \begin{bmatrix} v_{\alpha d} i_\alpha + v_{\beta d} i_\beta \\ v_{\beta d} i_\alpha - v_{\alpha d} i_\beta \end{bmatrix} \quad (8)$$

The direct active power p_d as follows:

$$p_d = v_{\alpha d} i_\alpha + v_{\beta d} i_\beta$$

$$= 3I_{d1}\cos(\varphi_{d1}) + \sum_{k=2}^{K} 3I_{dk}\cos\left((k-1)\hat{\theta}_d + \varphi_{dk}\right)$$

$$-\sum_{k=1}^{K} 3I_{qk}\cos\left((k\hat{\theta}_q + \hat{\theta}_d) + \varphi_{qk}\right) \quad (9)$$

By developing (9), direct active power components are,

$$p_d = \bar{p}_d + \tilde{p}_d + \tilde{p}_{dq} \quad (10)$$

With,

$$\bar{p}_d = 3I_{d1}\cos\varphi_{d1} \quad (11)$$

$$\tilde{p}_d = \sum_{k=2}^{K}[\cos(k-1)\hat{\theta}_d \quad \sin(k-1)\hat{\theta}_d] \times \begin{bmatrix} 3I_{dk}cos\varphi_{dk} \\ -3I_{dk}sin\varphi_{dk} \end{bmatrix} \quad (12)$$

$$\tilde{p}_{dq} = \sum_{k=2}^{K}[\cos\left(k\hat{\theta}_q + \hat{\theta}_d\right) \quad \sin\left(k\hat{\theta}_q + \hat{\theta}_d\right)] \times \begin{bmatrix} -3I_{qk}cos\varphi_{qk} \\ 3I_{qk}sin\varphi_{qk} \end{bmatrix} \quad (13)$$

Equation (10) can be written as a linear equation with a vector product as,

$$y = W^T X \quad (14)$$

With,

$$W = \begin{bmatrix} 3I_{d1}\cos\varphi_{d1} \\ -3I_{d1}\sin\varphi_{d1} \\ -3I_{q1}\cos\varphi_{q1} \\ 3I_{q1}\sin\varphi_{q1} \\ \vdots \\ 3I_{dk}\cos\varphi_{dk} \\ -3I_{dk}\sin\varphi_{dk} \\ -3I_{qk}\cos\varphi_{qk} \\ 3I_{qk}\sin\varphi_{qk} \end{bmatrix}; X = \begin{bmatrix} 1 \\ 0 \\ \cos(\hat{\theta}_q + \hat{\theta}_d) \\ \sin(\hat{\theta}_q + \hat{\theta}_d) \\ \vdots \\ \cos(k-1)\hat{\theta}_d \\ sin(k-1)\hat{\theta}_d \\ \cos(k\hat{\theta}_q + \hat{\theta}_d) \\ \sin(k\hat{\theta}_q + \hat{\theta}_d) \end{bmatrix} \quad (15)$$

ADALINE was first proposed by Widrow and Hoff who created learning algorithm for ADALINE (Widrow 1990). ADALINE is a single neuron structure with a linear activation function for multiple inputs and single output. The input vector X is composed of multiple sinusoidal signals of p_d, and the weight vector W is composed of the amplitudes of p_d, and y is the ADALINE output. Supervised learning algorithm is used to train the ADALINE. The ADALINE output y is compared to a desired value p_d.

The error,

$$\epsilon = p_d - y \quad (16)$$

By the Widrow-Hoff delta rule algorithm,

$$W(n+1) = W(n) + \Delta W(n) \quad (17)$$

With,

$$\Delta W(n) = \frac{\alpha\epsilon(n)X(n)}{\lambda + X^T(n)X(n)} \quad (18)$$

Where α is the learning rate, X(n) is the input vector at instant n, and λ is a constant to avoid division by zero.

Equation (16) is used to learn the ADALINE weights with help of equation (17) and reduces error. The stability and the speed of convergence are depending on choice of α between 0 and 1. The power amplitudes represented by W after training. W_1 is used to obtain $\bar{p}_d$ with k=1 i.e. fundamental component. Similarly, to estimate the q_d former ADALINE is used its desired output is obtained from equation (8) and after training, first weight vector is used to determine the average term $\bar{q}_d$.

In similar way, to estimate quadrature current components, quadrature voltages are

$$\begin{bmatrix} v_{\alpha q} \\ v_{\beta q} \end{bmatrix} = \begin{bmatrix} \cos(\hat{\theta}_q) \\ -sin(\hat{\theta}_q) \end{bmatrix} \quad (19)$$

C. ADALINE neural network for phase angle calculation

Consider the direct and quadrature current components given by,

$$i_d(t) = I_d \sin(\hat{\theta}_d + \varphi_d) \quad (20)$$

$$i_q(t) = I_q \sin(\hat{\theta}_q + \varphi_q) \quad (21)$$

The product $i_d(t).i_q(t)$ is,

$$i_d(t).i_q(t) = \frac{I_d.I_q}{2}\begin{pmatrix} \cos((\hat{\theta}_d - \hat{\theta}_q) + (\varphi_d - \varphi_q)) \\ -\cos((\hat{\theta}_d + \hat{\theta}_q) + (\varphi_d + \varphi_q)) \end{pmatrix} \quad (22)$$

or

$$i_d(t).i_q(t) = a_1\cos\left(\hat{\theta}_d - \hat{\theta}_q\right) - a_2\sin\left(\hat{\theta}_d - \hat{\theta}_q\right)$$

$$-a_3\cos\left(\hat{\theta}_d + \hat{\theta}_q\right) + a_4\sin\left(\hat{\theta}_d + \hat{\theta}_q\right) \quad (23)$$

With,

$$a_1 = \frac{I_d.I_q}{2}\cos(\varphi_d - \varphi_q) \quad (24)$$

$$a_2 = \frac{I_d.I_q}{2}\sin(\varphi_d - \varphi_q) \quad (25)$$

$$a_3 = \frac{I_d.I_q}{2}\cos(\varphi_d + \varphi_q) \quad (26)$$

$$a_4 = \frac{I_d.I_q}{2}\sin(\varphi_d + \varphi_q) \quad (27)$$

Equation (22) can be written as,

$$i_d(t).i_q(t) = W^T X \tag{28}$$

Which is a linear combination learned by an ADALINE neural network. Where W and X are given by,

$$W = \begin{bmatrix} a_1 \\ a_2 \\ a_3 \\ a_4 \end{bmatrix} = \frac{I_d.I_q}{2} \begin{bmatrix} \cos(\varphi_d - \varphi_q) \\ sin(\varphi_d - \varphi_q) \\ cos(\varphi_d + \varphi_q) \\ sin(\varphi_d + \varphi_q) \end{bmatrix} \tag{29}$$

$$X = \begin{bmatrix} cos(\hat{\theta}_d - \hat{\theta}_q) \\ -\sin(\hat{\theta}_d - \hat{\theta}_q) \\ -\cos(\hat{\theta}_d + \hat{\theta}_q) \\ \sin(\hat{\theta}_d + \hat{\theta}_q) \end{bmatrix} \tag{30}$$

The ADALINE is trained with equation (17) and the angular phase deduced from the first weight,

$$(\varphi_d - \varphi_q) = \arccos\left(\frac{2}{I_d.I_q} W_1\right) \tag{31}$$

4. SIMULINK MODEL AND SIMULATION RESULT

A. Hardware setup

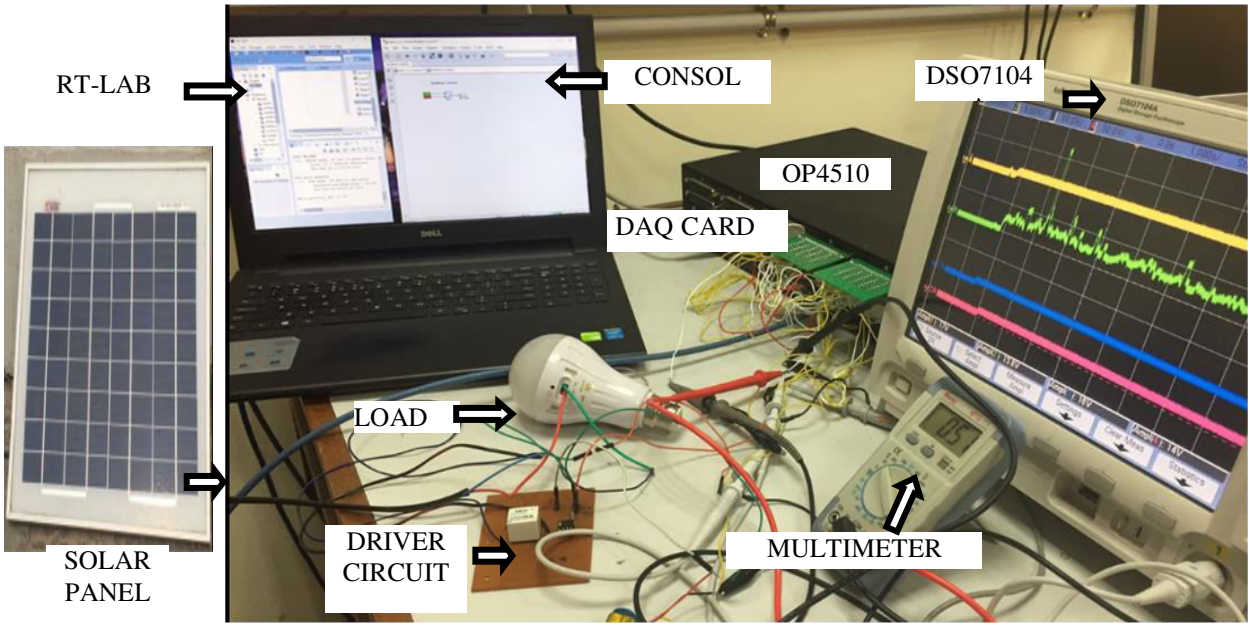

Figure-3. Hardware setup for proposed passive islanding detection.

Simulink model runs in OP4510 real-time simulator with the help of RT-LAB software on PC. Output from OP4510 is taken outside with the help of DAQ Cards and these outputs are displayed on DSO7104A. A driver circuit is used to isolate the load of 10W from the Solar Panel when islanding is detected. This LED bulb load powered by the solar panel of 10W, 22V which is present in outside environment. Driver circuit consists of optocoupler for electric isolation of circuit and relay for switching operation. In normal condition LED bulb glows as there is no islanding. When islanding occurs, islanding signal goes high (+5V) at that time relay disconnects load from solar panel. i.e. islanding detection and prevention.

B. System under study

The system under study is a grid connected hybrid wind PV system. It consists of a hybrid wind PV system connected to grid through circuit breaker and a RLC Load is connected at the point of common coupling (PCC).

C. Islanding detection unit

In Phase angle based IDT, change in phase angle is detected from PCC voltage and current using PLL and ADALINE algorithm. In algorithm phase angle is converted in degree. Real part of estimated complex phase angle is compared with a threshold limit by carefully observing the change in phase angle and set to 42000. The comparator output is send to the counter to count the change in phase angle exceeding threshold limit. When a certain number is reached in counter for 5, islanding signal is generated i.e. signal goes from logic 0 to logic 1. For RMS current based IDT, change in RMS current is compared with the threshold limit similar to phase angle based IDT. RMS current signal is obtained from Figure-2 strategy.

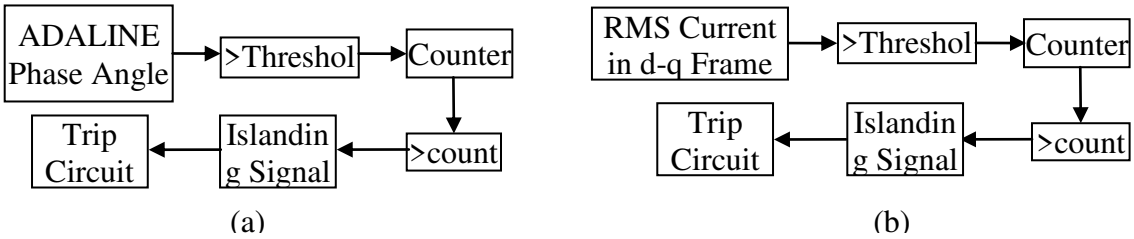

Figure-4. Islanding detection unit for (a) Change in phase angle and (b) Change in RMS current.

D. SIMULINK and OP4510 real-time simulator result

OP4510 real-time simulator is used to implement a new PIDT based on change in RMS current in d-q frame. Proposed method is compared with change in phase angle using ADALINE in [37]. Four general cases are considered to study the performance of proposed PIDT, these cases are as follows:

Case I: 10KW load with U.P.F.
Case II: 10KW load with 0.75 lagging P.F.
Case III: 10KW load with 0.7 leading P.F.
Case IV: Load Dynamics

Case I: U.P.F. Load

In this case a 10KW unity power factor load is considered to simulate the proposed PIDT. Figure-5(a) shows changes in phase angle and Figure-5(b) islanding signal when a fault occurs at 0.2sec. At fault occurrence simulation result are shown as it takes 30msec for islanding signal to change from 0 to 1. Figure-5(c) evaluates the PIDT using RMS current in d-q frame. It detects islanding in 40msec as shown in Figure-5(d). While MATLAB/SIMULINK model has been implemented and evaluated using OP4510 Real-time simulator. Output waveform at DSO4710A is shown in Figure-6. Phase angle based PIDT takes 30msec and RMS current based PIDT takes 160msec to detect islanding when a random fault occurs as shown in Figure-6.

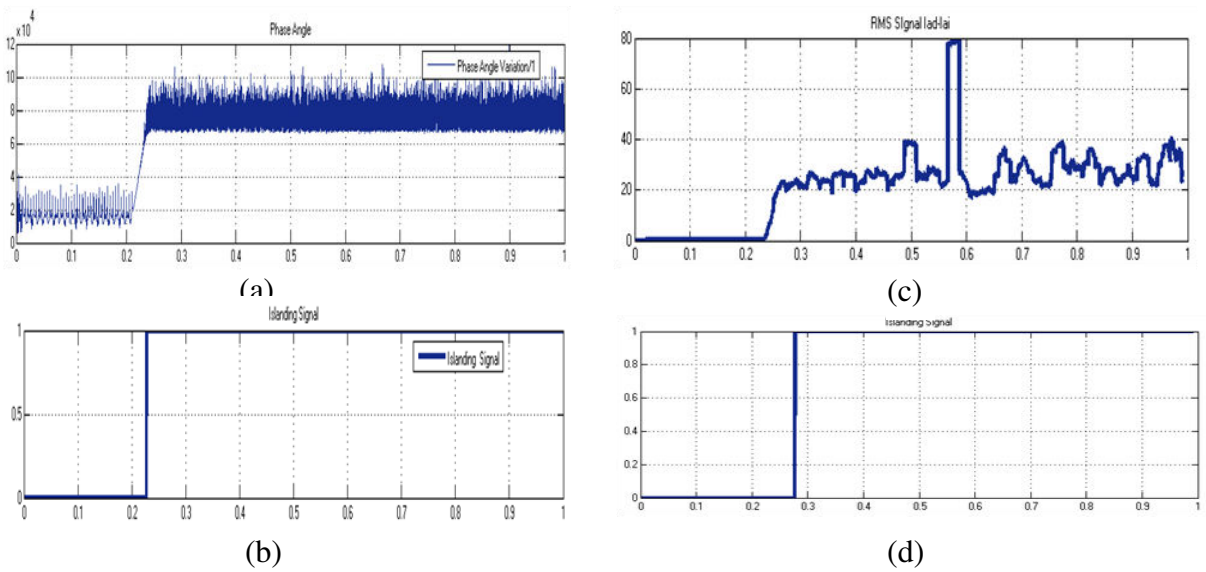

Figure-5. SIMULINK waveform for a 10KW load at unity power factor (a) Change in phase angle, (b) Islanding signal for phase angle, (c) Change in RMS current and (b) Islanding signal for RMS current.

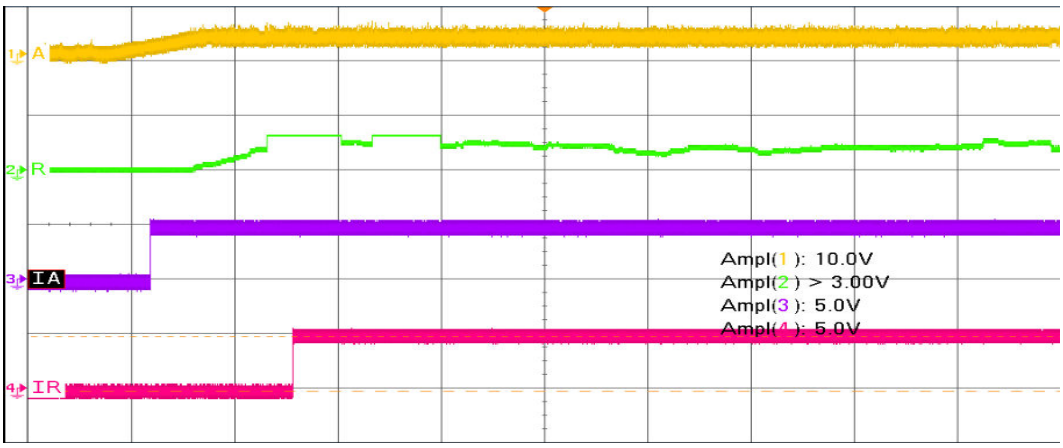

Figure-6. OP4510 waveform display (where A- Change in phase angle, R- change in RMS current, IA- islanding signal for A, IR- islanding signal for R) for a 10KW load at unity power factor

Case II: Lagging power factor

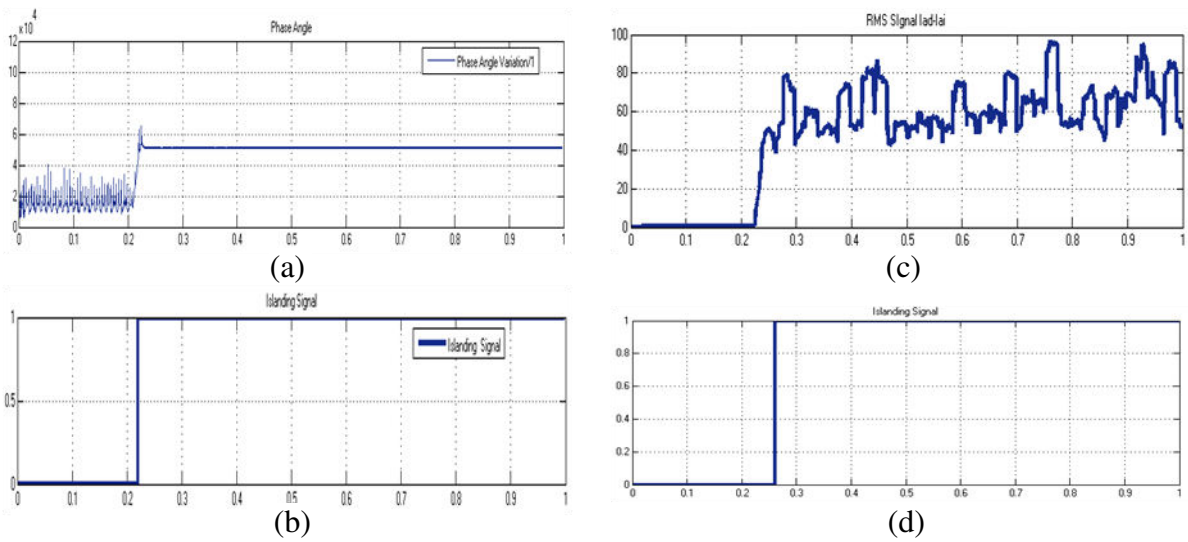

Figure-7. SIMULINK waveform for a 10KW load at 0.75 lagging power factor (a) Change in phase angle (b) Islanding signal for phase angle, (c) Change in RMS current and (d) Islanding signal for RMS current

In this case a 10KW, 0.75 lagging power factor load is considered to simulate the proposed PIDT. Figure-7(a) shows change in phase angle and Figure-7(b) islanding signal when a fault occurs at 0.2sec. At fault occurrence simulation result are shown as it takes 30msec for islanding signal to change from 0 to 1. Figure-7(c) evaluates the PIDT using RMS current in d-q frame. It detects islanding in 35msec as in Figure-7(d). While MATLAB/SIMULINK model has been implemented and evaluated using OP4510 Real-time simulator. Output waveform at DSO4710A is shown in Fig.8. Phase angle based PIDT detects false islanding and RMS current based PIDT takes 200msec to detect islanding when a random fault occurs as shown in Figure-8.

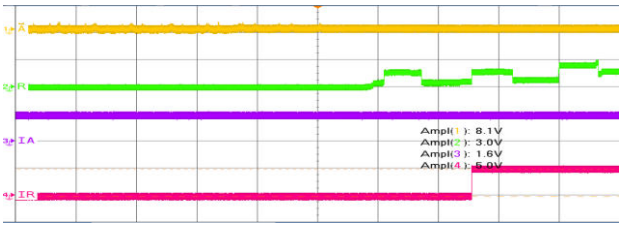

Figure-8. OP4510 waveform display (where A- change in phase angle, R- change in RMS current, IA- islanding signal for A, IR- islanding signal for R) for a 10KW Load at 0.75 lagging power factor.

Case III: leading power factor

In this case a 10KW, 0.7 leading power factor load is considered to simulate the proposed PIDT. Figure-9(a) shows change in phase angle and Figure-9(b) islanding signal when a fault occurs at 0.2sec. At fault

occurrence simulation result are shown as it takes 25msec for islanding signal to change from 0 to 1. Figure-9(c), (d) evaluates the PIDT using RMS current in d-q frame. it detects islanding in 40msec.

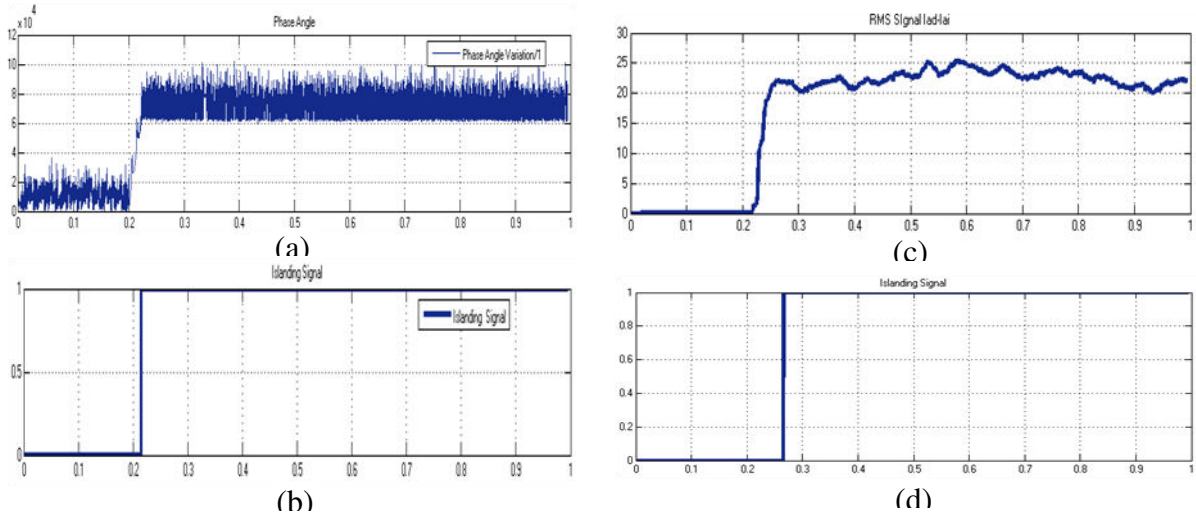

Figure-9. SIMULINK waveform for a 10KW Load at 0.7 leading power factor (a) Change in phase angle (b) Islanding signal for phase angle, (c) Change in RMS current and (d) islanding signal for RMS current

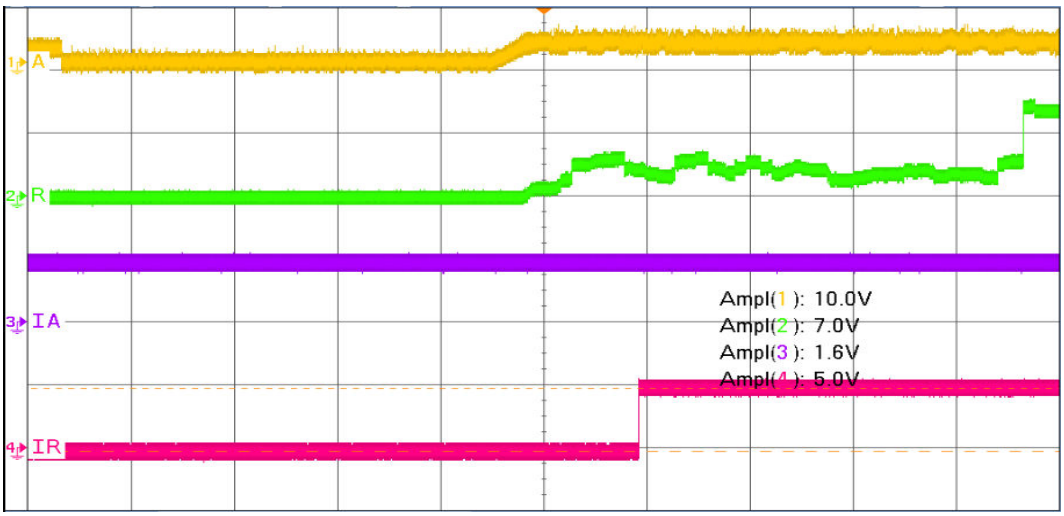

Figure-10. OP4510 waveform display (where A- change in phase angle, R- change in RMS current, IA- islanding signal for A, IR- islanding signal for R) for a 10KW load at 0.75 lagging power factor.

While MATLAB/SIMULINK model has been implemented and evaluated using OP4510 Real-time simulator. Output waveform at DSO4710A is shown in Figure-10. Phase angle based PIDT false detected and RMS current based PIDT takes 140msec to detect islanding when a random fault occurs as shown in Figure-10. Table-1 shows the comparison of five different load cases for both phase angle and RMS current based islanding detection techniques.

Table-1. Comparison between SIMULINK and OP4510 results for phase angle and RMS current based PIDT.

PIDT/ Load	Phase angle based islanding detection (msec) [37]		RMS current based islanding detection (msec)	
	SIMULINK	OP4510	SIMULINK	OP4510
U.P.F	20-25	30	40	160
0.75 Lag	20-25	x	35	200
0.7 Lead	20-25	x	40	140
0.85 Lag	20-25	x	50	160
0.85 Lead	20-25	x	45	170

Where x- false detection

Case IV: Load dynamics

In this case load switching is done rapidly and a random fault is generated. When load is switched from 10KW, U.P.F. to 10KW, 0.85 lagging power factor, response of proposed change in phase angle and RMS current PIDT is shown in Figure-11. Phase angle based islanding technique detects islanding when load changes while PIDT based on RMS current detects islanding on occurrence of fault.

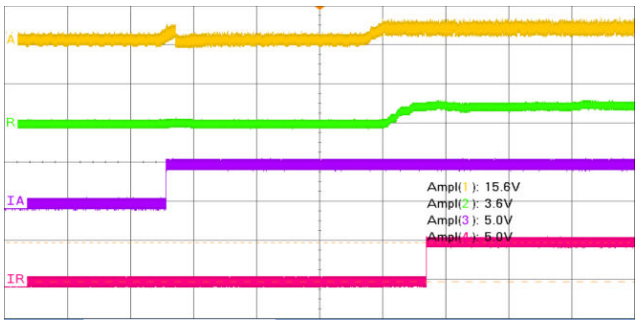

Figure-11. OP4510 waveform display (where A- change in phase angle, R- change in RMS current, IA- islanding signal for A, IR- islanding signal for R) for load dynamics.

CONCLUSION AND FURTURE SCOPE

An effective ADALINE algorithm for passive islanding detection using change in RMS current estimation in d-q frame is proposed in the study. Proposed PIDT is compared with change in phase angle based on ADALINE in [37]. The proposed algorithm is validated using Op4510 real-time simulator (hardware in loop). HIL results shows that the change in RMS current based PIDT detects islanding in 140msec to 200msec while phase angle based PIDT detects false islanding in case of load switching and different power factor. As for proposed PIDT threshold limits are selected based on 1 sec simulation and then SIMULINK model is used in real-time environment there is change in islanding detection from 40msec to 200msec. Islanding detection is also affected by hardware sampling rate while implementation. So future work can be done in this area to reduce islanding detection time.

ACKNOWLEDGEMENT

I would like to express my sincere gratitude to National Institute of Technical Teachers Training and Research, Chandigarh (MHRD) for providing the opportunity to carry out this present thesis work.

COMPLIANCE WITH ETHICAL STANDARDS

No Funding.

CONFLICT OF INTEREST

The authors declare that they have no conflict of interest.

REFERENCES

[1] Qahouq J. A. A., Jiang Y. and Orabi M. 2014. MPPT Control and Architecture for PV Solar Panel with Sub-Module Integrated Converters, Journal of Power Electronics. 14(6): 1281-1292.

[2] Park S. J., Lee H. S., Kim C. I., Park J. H., Jeon H. J. and Ryeom J. 2013. Controller Design of a Novel Power Conditioning System with an Energy Storage Device for Renewable Energy Sources under Grid-connected Operation, Journal of Power Electronics. 13(3): 390-399.

[3] Akyuz E., Oktay Z. and Dincer I. 2012. Performance Investigation of Hydrogen Production from a Hybrid Wind-PV System, International Journal of Hydrogen Energy. 37(27): 16623-16630.

[4] Hakimi S. M., and Moghaddas-Tafreshi S. M. 2009. Optimal Sizing of a Stand-alone Hybrid Power System via Particle Swarm Optimization for Kahnouj Area in South-East of Iran, Renewable Energy. 34(7): 1855–1862.

[5] Rehman S., Alam M. M., Meyer J. P., and Al-Hadhrami L. M. 2012. Feasibility Study of a Wind-

PV-diesel Hybrid Power System for a Village, Renewable Energy. 38(1): 258–268.

[6] Chowdhury S. P., Chowdhury S., and Crossley P. A. 2011. UK scenario of islanded operation of active distribution networks with renewable distributed generators. International Journal Electrical Power Energy System. 33(7): 1251-1255.

[7] Balaguer I.J., Lei Q., Yang S., Supatti U. and Fang Z. P. 2011. Control for grid connected and intentional islanding operations of distributed power generation, IEEE Transaction on Industrial Electronics. 58(1): 147–157.

[8] UL1741, Inverter, converter, and controllers for use in independent power system.

[9] IEEE P1547.1TM. 2005. IEEE standard conformance test procedures for equipment interconnecting distributed resources with electric power systems 1547.1.

[10] IEEE Std. 929-2000. IEEE recommended practice for utility interface of photovoltaic (PV) systems.

[11] Mango F. D., Liserre M., Aquila A. D. and Pigazo A. 2006. Overview of anti-islanding algorithms for PV systems. Part I: Passive methods, Power Electronics and Motion Control Conference, Portoroz, Slovenia. 1878-1883.

[12] Mozina C. J. 2001. Interconnection protection of IPP generators at commercial/ industrial facilities. IEEE Transaction on Industrial Application. 37(3): 681-688.

[13] Affonso C. M., Freitas W., Xu W., and da Silva L. C. P., (2005). Performance of ROCOF relays for embedded generation applications, IEE Proceedings-Generation Transmission Distribution. 152(1): 109-114.

[14] Geng H., Xu D., Wu B. and Yang G. 2011. Active islanding detection for inverter-based distributed generation systems with power control interface. IEEE Transaction Energy Conversion. 26(4): 1063-72.

[15] Mango F. D., Liserre M. and Aquila A. D. 2006. Overview of anti-islanding algorithms for PV system. Part II: Active methods. Power Electron Motion Control Conference, Portoroz, Solvenia. 1884-1889.

[16] Hung G. K., Chang C. C. and Chen C. L. 2003. Automatic phase-shift method for islanding detection of grid-connected photovoltaic inverters. IEEE Transaction Energy Conversion. 18(1): 169-173.

[17] Huang S. J., and Pai F. S. 2001. Design and operation of grid-connected photovoltaic system with power-factor control and active islanding detection. IEE Proceeding- Generation Transmission Distribution. 148(3): 243-250.

[18] Ropp M. E., Begovic M., Rohatgi A., Kern G. A., Bonn R. H., and Gonzalez S. 2000. Determining the relative effectiveness of islanding detection methods using phase criteria and non-detection zones. IEEE Transaction on Energy Conversion, 15(3): 290-296.

[19] Kobayashi H., and Takigawa K. 1994. Statistical evaluation of optimum islanding preventing method for utility interactive small scale dispersed PV systems, Proceeding of 1st WCPEC, Waikoloa, HI, USA, 1085–1088.

[20] Bahrani B., Karimi H. and Iravani R. 2011. Non-detection zone assessment of an active islanding detection method and its experimental evaluation. IEEE Transaction Power Delivery. 26(2): 517-525.

[21] Ropp M. E., Aaker K., Haigh J. and Sabbah N. 2000. Using power line carrier communications to prevent islanding of PV power systems. IEEE Photovoltaic Specialists Conference, Anchorage, AK, USA. 1675-1678.

[22] Ropp M., Larson D., Meendering S., Mcmahon D., Ginn J., Stevens J., Bower W., Gonzalez S., Fennell K. and Brusseau L. 2006. Discussion of a power line carrier communications-based anti-islanding scheme using a commercial automatic meter reading system. IEEE Photovoltaic Energy Conversion Conference, Waikoloa, HI, USA. 2351-54.

[23] Akagi H., Watanabe E. H., and Aredes M. 2007. Instantaneous Power Theory and Applications to Power Conditioning, Hoboken. NJ:Wiley/IEEE.

[24] Nguyen N. K., Flieller D., Wira P. and Abdeslam D. 2009. Neural network for phase and symmetrical components estimation in power systems, in Proc. 35th Annual Conference IEEE Industrial Electronics Society, Porto, Portugal. 3-5.

[25] Bose B. K. 2007. Neural network applications in power electronics and motor drives-an introduction and perspective, IEEE Transaction on Industrial Electronics. 54(1): 14-33.

[26] Fayyad Y. and Osman A. 2010. Neuro-wavelet based islanding detection technique. IEEE Electric Power and Energy Conference, Halifax, NS, Canada. 1-6.

[27] ElNozahy M. S., El-Saadany E. F. and Salama M. M. A. 2011. A robust wavelet-ANN based technique for islanding detection, IEEE Power and Energy Society General Meeting, Detroit, MI, USA. 1-8.

[28] Abd-Elkader A. G., Allam D. F., and Tageldin E. 2014. Islanding detection method for DFIG wind turbines using artificial neural networks. International Journal of Electrical Power and Energy System. 62, 335-343.

[29] Girgis A. A., Chang W. B. and Makram E. B. 1991. A digital recursive measurement scheme for online tracking of harmonics. IEEE Transaction on Power Delivery. 6, 1153-1160.

[30] Bettayed M. and Qidai U. 1998. Recursive estimation of power system harmonics. Electrical Power Systems Research. 47, 143-152.

[31] Pradhan A. K., Routray A. and Basak A. 2005. Power system frequency estimation using least mean square technique. IEEE Transaction on Power Delivery. 20, 1812-1816.

[32] Dash P. K., Swain D. P., Liew A. C. and Rahman S. 1996. An adaptive linear combiner for on-line tracking of power system harmonics. IEEE Transaction on Power System Harmonics. 11, 1730-1735.

[33] Bettayed M. and Qidai U. 2003. A Hybrid Least Squares-GA-based algorithm for harmonic estimation, IEEE Transactions on Power Delivery. 18, 377-382.

[34] Joorabian M., Mortazavi S. S. and Khayyami A. A. 2008. Harmonic estimation in a power system using a novel hybrid least square- Adaline algorithm, Electric Power Systems Research. 79, 107-116.

[35] Sarkar A., Choudhury S. R. and Sengupta S. 2011. A self-synchronized ADALINE network for on-line tracking of power system harmonics, Measurement. 44, 784-790.

[36] Marie M., Saadany F. and Salama M. 2004. A processing unit for symmetrical components and harmonics estimation based on a new adaptive linear combiner structure. IEEE Transactions on Power Delivery. 19, 1245-1252.

[37] Al-Wadie M. O., Diab H. Y. and Helw H. M. E. 2013. Simulation of Islanding Detection Scheme Based On Fast Angle Estimation Method for Grid Connected Photovoltaic Systems Using ADALINE Technique. UKSim 15th International Conference on Computer Modelling and Simulation, Cambridge, UK. 548-553.

[38] Yousfi F. L., Abdeslam D. O. and Nguyen N. K. 2010. Adaline for fault detection in electrical high voltage transmission line, 36th Annual Conference on IEEE Industrial Electronics Society, Glendale, AZ, USA. 1963-1968.

[39] Yousfi F. L., Abdeslam D. O., Bouthiba T., Nguyen N. and Mercklé J. 2012. Adaline for Online Symmetrical Components and Phase-Angles Identification in Transmission Lines. IEEE Transactions on Power Delivery. 27(3): 1134-1143.

[40] Widrow B. and Lehr M. A. 1990. 30 years of adaptive neural networks: Perceptron, Madaline, and Back Propagation. Proceeding of IEEE. 79(9): 1415-1442.